

Load-relaxation testing at elevated strain rates

D. W. HENDERSON, R. C. KUO, C.-Y. LI

Department of Materials Science and Engineering, Cornell University, Ithaca, New York 14853, USA

The feasibility of a new mechanical testing technique is described. This technique allows the collection of load-relaxation type data at higher strain rates than is possible in a conventional load-relaxation test. This technique was used on commercial purity aluminium and 304 stainless steel at strain rates up to 5 sec^{-1} . Good agreement with Hart's state variable model for plastic deformation was found.

1. Introduction

One approach in characterizing the plastic deformation properties of a material is to measure the plastic strain rate, $\dot{\epsilon}$, produced as a function of the imposed stress, σ . From the standpoint of interpreting such measurements, it is often desirable that the data be collected under conditions where the microstructural state of the material is maintained essentially unchanged. However, most mechanical testing methods impose a significant amount of plastic deformation on the specimen during the test. Thus, the microstructural (plastic) state of the material is constantly evolving throughout the test due to strain hardening effects. The load-relaxation test is an exception in that the incremental plastic strain imposed on the material during the test can be made negligibly small. Therefore, the stress-plastic strain rate relationship, $\dot{\epsilon}(\sigma)$, for the material in a particular microstructural or plastic state can be directly measured over a range of strain rate.

Most conventional mechanical testing, including load relaxation testing, has been performed at low strain rates (10^{-9} to 10^{-2} sec^{-1}). However, metal-forming processes typically involve medium (10^{-2} to 10^{+2} sec^{-1}) to high (10^{+2} to 10^{+6} sec^{-1}) strain rates. A variety of mechanical testing techniques have been developed for testing in these higher strain-rate ranges. At medium strain rates, the cam plastometer [1-5] and other constant strain rate or constant displacement rate techniques have been utilized [6-10]. At high strain

rates a number of testing techniques have been developed, the most notable of which is a split Hopkinson bar technique [11-13]. All of these techniques involve the imposition of significant plastic deformation during the testing procedure. None of these techniques has been used to directly measure the $\dot{\epsilon}(\sigma)$ relationship for a particular plastic state of a material at medium or high strain rates.

This paper discusses an extension of the basic principle of the load-relaxation test to medium strain rates using conventional tensile testing equipment. While load-relaxation testing can be performed in tension, compression, and torsion, only the case of uniaxial tension will be discussed in detail in this paper. Testing using the other states of stress involves completely analogous considerations.

2. The load-relaxation test

The principles of the load-relaxation test have been outlined by Hart [14] and Lee and Hart [15] in two papers on uniaxial testing. As such and in order to maintain consistency, their notation will be adopted in the following development. With reference to Fig. 1, L is defined as the instantaneous plastic length of the specimen which had an initial length, L_0 . L_1 is defined as the position of the moving member of the testing machine, and this length is measured from a fixed point chosen in such a way that $L_1 = L_0$ at the beginning of the test. At any particular time during the test,

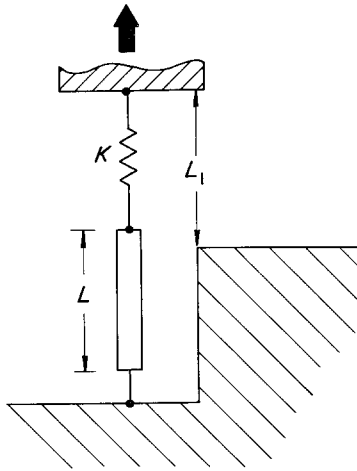


Figure 1 Schematic representation of a tensile testing machine with a specimen of plastic length, L , and a machine stiffness, K .

$L_1 = L_0 + X$, where X is the displacement of the moving member from the initial position. P is defined as the instantaneous load supported by the specimen and load train.

The elastic characteristics of the load train are such that the load, P , is related to the elastic elongation of the load train by

$$P = K(L_1 - L), \quad (1)$$

where K is the elastic spring constant of the load train. Equation 1 is a quasistatic approximation; the criteria for its validity are examined in the Appendix for the present application. Evaluation of these criteria indicates that Equation 1 is a good approximation for the experiments described below.

The load-relaxation test is usually performed by loading the specimen under a constant displacement rate, \dot{X} , until a desired plastic length, L , is reached. The moving member of the machine is then stopped, but the specimen continues to elongate under the elastically supported load of the load train, and the load relaxes in a continuous manner as the specimen elongates. The load and specimen length can be directly measured as a function of time during the relaxation. If K is sufficiently large, only a very small additional elongation of the specimen is required to produce a large decrease in load. Thus, a large span of the $\dot{\epsilon}(\sigma)$ relationship can be directly determined for the material in a particular plastic state. Differentiating Equation 1 and substituting $L\dot{\epsilon}$ for \dot{L} yields

$$\frac{\dot{P}}{K} + L\dot{\epsilon} = \dot{L}_1, \quad (2)$$

where the dot over the variable indicates the first derivative of that variable with respect to time. If the movable member of the testing machine is fixed during the load relaxation, $\dot{L}_1 = 0$. This is the conventional procedure in load-relaxation testing and for the sake of clarity this case will be referred to as a static load-relaxation.

Equation 2 can be solved for the time interval associated with a load-relaxation between two strain rates of interest if the $\dot{\epsilon}(\sigma)$ relation is known. It is important to note that this time interval can be quite short for a static load-relaxation test at medium and high strain rates, if a conventional specimen geometry and a typical load train spring constant are used. For instance, for annealed commercial purity aluminium with approximately 10% strain, a specimen with a 2.54 cm (1 in.) gauge length, a 0.635 cm (0.25 in.) gauge diameter, has a relaxation time of approximately $15 \mu\text{sec}$ for the strain rate to drop from 10 to 1sec^{-1} at room temperature. This time interval was calculated for a load train spring constant, K , equal to $4.4 \times 10^5 \text{ N m}^{-1}$ ($5 \times 10^4 \text{ lb in.}^{-1}$).

Physically, this result obtains because a very small stress drop in this material produces an enormous change in strain rate and this stress drop occurs very rapidly at these strain rates. In order to perform a static load-relaxation test in this strain rate range, the moving member of the tensile machine must be decelerated from high velocities and fixed in position in a time interval which is short compared to $15 \mu\text{sec}$. Such a rapid deceleration is simply not feasible with conventional testing equipment. Even if such a deceleration process were feasible, the time intervals involved would place an enormous demand on any data acquisition system.

There are two possible avenues of approach in trying to circumvent the problem. One approach is to modify the specimen geometry and load train constant in such a way as to increase the load-relaxation time. For some materials in certain temperature ranges this may be a viable solution. But, the modifications required make such an approach unwieldy as a universal solution because the elastic elongation of the load train would have to approach the specimen length, L_T , for material/temperature regimes such as that for aluminium cited above.

The other approach is to relax the condition that $\dot{L}_1 = 0$ during the load relaxation. In this method the load and specimen elongation are

simultaneously measured throughout the rapid deceleration of the moving member of the testing machine. During this deceleration, the specimen is swept through a considerable range in strain rate as the load relaxes. It may thus be termed a dynamic load-relaxation test. However, it is still possible to impose only a small amount of additional plastic deformation on the specimen during the test. The test results should have the same meaning and importance as data obtained in a conventional static load-relaxation test. This second method is the approach which was initially taken and which is reported here.

3. The dynamic load-relaxation test

Although screw driven tensile testing machines have been used extensively at low strain rate for static load-relaxation experiments [16], these machines are typically not capable of speeds greater than approximately 0.5 in. sec^{-1} . Therefore, attention will be directed to the use of closed control loop hydraulic machines because of their higher speeds ($\sim 500 \text{ in. sec}^{-1}$). Hydraulic machines have the added advantage that the stopping behaviour for L_1 as a function of time can be controlled over a broader range of adjustment than for screw-driven machines.

There are two ways to decelerate the actuator of a closed control loop hydraulic machine in performing a dynamic load relaxation which merit consideration. The method which perhaps produces the most rapid deceleration is to pull the actuator into a mechanical stop. The other method involves using the hydraulic control system to affect the actuator deceleration. This second method was initially examined and will be reported

here. Fig. 2 shows qualitatively the desired characteristic shape for the displacement L_1 as a function of time for a dynamic load-relaxation test using the hydraulic control system to decelerate the actuator. The actuator position, L_1 , is initially equal to L_0 . The actuator is then rapidly accelerated to a high speed and that speed is maintained approximately constant until the desired value of L_1 is achieved. The actuator is then rapidly decelerated to zero velocity, i.e. $\dot{L}_1 = 0$. As shown in fig. 2, both the gain and the damping in the control loop are adjusted to give a very sharply peaked behaviour. The best (the sharpest) is produced with the control loop adjusted to produce an underdamped control behaviour. Thus, the initial peak in L_1 is followed by a series of damped oscillations. The amount of initial "fall back" of the actuator, ΔL_1 , may indeed be larger than the total elastic elongation of the load train. Therefore, in order to avoid placing the specimen under compression, "slack" grips must be used which will support only tensile forces.

Fig. 3 shows a schematic drawing of the total specimen length, L_T , as a function of time which is produced by an L_1 behaviour shown in Fig. 2 using "slack" grips. It should be noted that L_T is the sum of the plastic length, L , the anelastic elongation and the elastic elongation of the test specimen, and as such, L_T is the quantity which is directly measured during the test. The "spring back", ΔL_T , after the peak in L_T is due in part to elastic and/or anelastic recovery upon unloading the specimen.

Also shown in Fig. 3 is a schematic representation of the load, P , simultaneously measured with the total specimen length, L_T . It can be seen

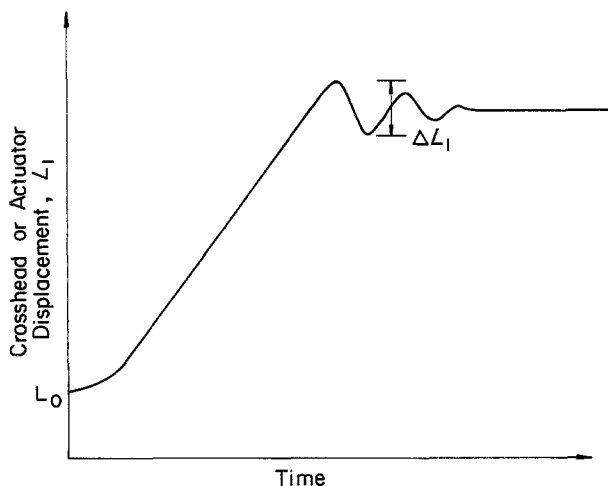


Figure 2 Schematic drawing of actuator displacement as a function of time using hydraulic control system to affect a rapid deceleration of moving actuator.

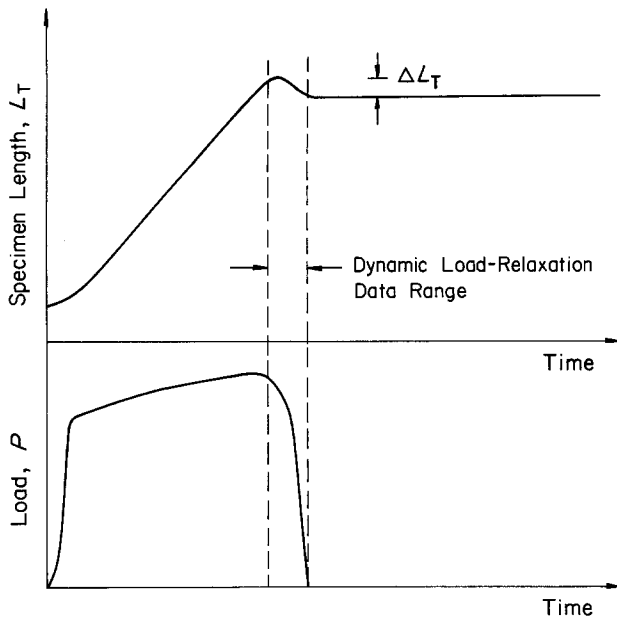


Figure 3 Schematic representation of specimen length as a function of time and load as a function of time for dynamic load-relaxation test.

that near the peak in L_T , where the total strain rate is decreasing rapidly, the load, P , decreases significantly in accordance with the changing strain rate. If the L_T behaviour is sharply peaked, then a considerable range of strain rate is sampled with very little additional plastic elongation of the specimen in the neighbourhood of this peak. The plastic length, L , can be computed by subtracting the elastic elongation from L_T , and by taking proper account of the anelastic contribution. Based on the work-hardening characteristic of the material, a criterion must be established for the maximum change in length ΔL which can be allowed during the dynamic load relaxation without significantly changing the microstructural state of the material. The span, ΔL , measured back from the final experimental value for L corresponds to the time span of data to be used in computing the $\dot{\epsilon}(\sigma)$ behaviour for this "constant microstructural or plastic state". In general, in order to obtain a usable strain rate range of significant size, the amount of plastic deformation which must be tolerated is greater than that typically found in the static load-relaxation test at low strain rates. How much greater will depend on the rapidity of the stopping transient.

If \dot{L}_1 is large for most of the period during which the initial strain is imposed on the specimen preceding the dynamic load-relaxation, then the total time required for the experiment is quite short. For an average actuator velocity of 200 cm sec^{-1} ($\sim 40 \text{ in. sec}^{-1}$), a specimen with a 2 cm ($\sim 0.8 \text{ in.}$)

gauge length would be subjected to a 50% true strain in approximately 13 msec.

The energy required to plastically deform the specimen is in large measure converted to heat and the temperature of the specimen will rise throughout the straining process. This temperature rise is not trivial and must be taken into account. However, the temperature rise during the dynamic load relaxation itself is quite small and can, in general, be neglected. The short time frame for a dynamic load-relaxation test (including the preliminary strain and the dynamic load relaxation) ensures that very little heat is lost for the system and the heat generated by the plastic deformation can be assumed to remain in the specimen. However, the dynamic load relaxation itself can be viewed as an adiabatic experiment performed at a temperature which has been elevated by the preliminary strain.

4. Experiments

4.1. Materials preparation

Initial dynamic load-relaxation testing was conducted on commercially pure aluminium and on 304 stainless steel.

The commercial purity aluminium test specimens were machined from swaged rod stock. The tensile specimens were annealed in a vacuum furnace at 500°C for 1 h and then cooled slowly to room temperature. The grain size estimated by the circle-intercept procedures was $114 \pm 7 \mu\text{m}$.

The 304 stainless steel specimens were machined

from rod stock and vacuum annealed at 1200°C for 5 min. The test specimens were then rapidly cooled to room temperature in a stream of helium gas. The microstructure consists of equiaxed grains containing annealing twins and the grain size was $87 \pm 10 \mu\text{m}$.

All test specimens had a 3.18 cm (1.25 in.) gauge length and a standard ASTM geometry for round tensile testing specimens was used. The aluminium specimens had a gauge diameter of 0.64 cm (0.25 in.) and the 304 stainless steel specimens had a gauge diameter of 0.254 cm (0.100 in.).

4.2. Mechanical testing and measurement systems

A MTS hydraulic testing machine with closed loop control and a standard hydraulic valve was used. The maximum actuator velocity was 38 cm sec^{-1} (15 in. sec^{-1}). While the load frame, actuator, and valve system were not optimally designed for dynamic load-relaxation experiments, the available system was utilized to demonstrate the feasibility of this type of testing procedure.

The elongation of the test specimen as a function of time was directly measured using a pair of MTI capacitance gauges. The displacement-voltage transfer function for these devices is substantially independent of frequency up to 2000 Hz. This frequency is well above any of the important Fourier frequency components of the plot of

displacement against time measured during the tests.

A Kistler piezoelectric force link was used to measure load. The resonant frequency of the force link with the upper specimen grip and capacitance gauges mounted was in excess of 10 kHz. This frequency is higher than the frequencies of any of the significant Fourier components of the plot of measured load against time.

Because of the need for very rapid load and displacement data acquisition, a Nicolet 4094 digital storage oscilloscope was used. Typically, data was acquired at a rate of $5 \times 10^4 \text{ points sec}^{-1}$ with 12 bit accuracy. The data were analysed with a minicomputer to yield the stress-nonelastic strain rate data described below.

All experiments were carried out at room temperature.

4.3. Experimental results and discussion

Fig. 4 shows typical data obtained from a dynamic load-relaxation test performed on commercially pure aluminium. Sample load and elongation are plotted as a function of time for the entire testing procedure. Only data which was measured between the indicating arrows (a 1.7 msec interval) on the time axis was used in computing the $\dot{\epsilon}(\sigma)$ relationship during the dynamic load relaxation. The additional plastic deformation which was imposed on the specimen during this time was 0.5%, and the measurable non-elastic strain rate range

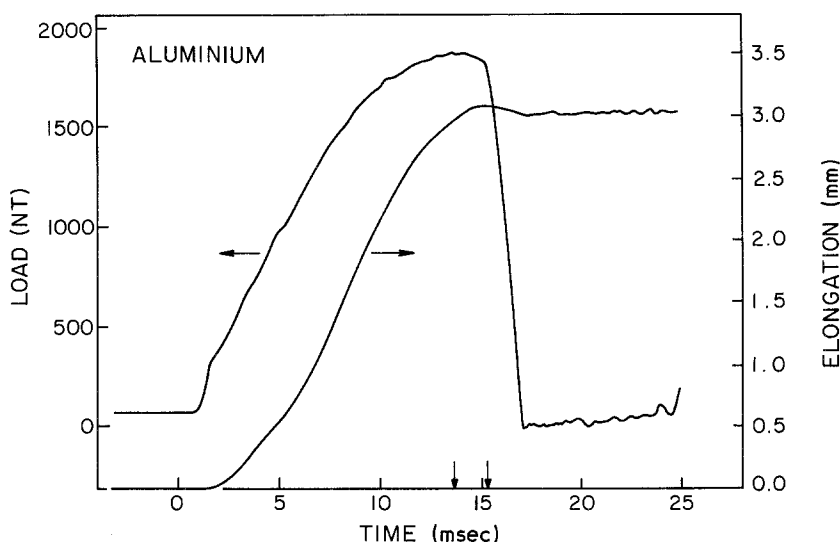


Figure 4 Curves of experimentally measured load plotted against time and specimen elongation plotted against time for commercial purity aluminium in a dynamic load-relaxation test.

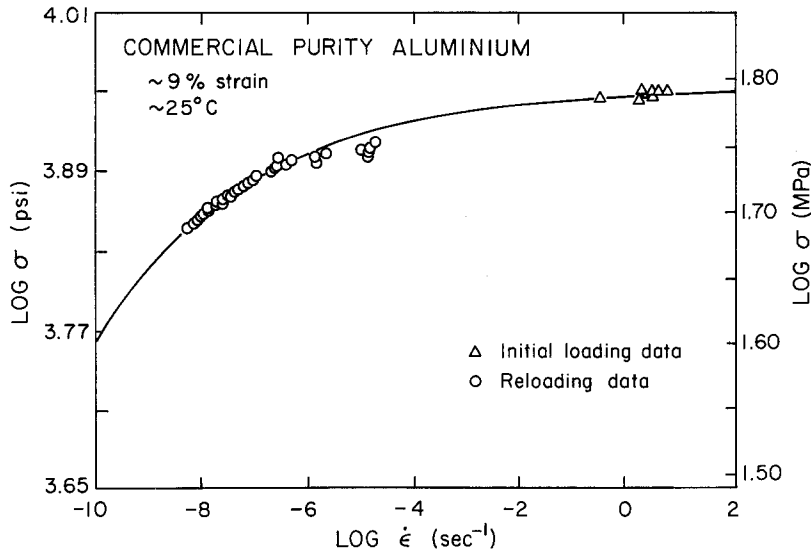


Figure 5 Log stress against log strain rate curve for commercial purity aluminium. Data shown for a constant plastic state. Solid line shows best low strain-rate fit for Hart's model.

spanned 1.5 orders of magnitude from approximately 5 to 0.15 sec^{-1} . The $\dot{\epsilon}(\sigma)$ relationship is shown in the form of a plot of $\log \sigma$ against $\log \dot{\epsilon}$ in Fig. 5. Also shown in Fig. 5 is the data obtained by remeasuring the same specimen with a static load-relaxation test at lower strain rates (10^{-3} to 10^{-8} sec^{-1}). This second test was performed by remounting the same specimen in an Instron screw-driven tensile machine. Because very little additional plastic strain was imposed on the sample in this second measurement, the plastic state of the material was essentially unchanged and thus both sets of measurements characterize the same plastic state. The appropriate equation from Hart's state variable model [17] was fitted to the low strain-rate data. Specifically, the $\dot{\epsilon}(\sigma)$ relationship in Hart's model at high homologous temperatures and low strain rates is given by

$$\ln \left(\frac{\sigma^*}{\sigma} \right) = \left(\frac{\dot{\epsilon}^*}{\dot{\epsilon}} \right)^\lambda, \quad (3)$$

where σ^* is called the hardness and is a measure of the plastic state of the material, λ is an adjustable parameter but is always found to be approximately equal to 0.15, $\dot{\epsilon}^*$ is a rate parameter. Both σ^* and $\dot{\epsilon}^*$ were treated as adjustable parameters in fitting the low strain rate data. The equation of the form of Equation 3, which best fits the low strain rate data, is plotted in Fig. 5 as a solid line. It is clear that this equation also describes very well the data obtained at medium strain rates in the dynamic load-relaxation test.

Fig. 6 shows typical load and elongation data for 304 stainless steel which was obtained in a dynamic load-relaxation test. It is apparent that the load data is significantly noisier than that for aluminium and it is probable that the oscillatory nature of the load signal is due to increased vibration of the load frame caused by a more abrupt initial increase in load in the 304 stainless steel sample. The $\dot{\epsilon}(\sigma)$ relationship obtained from the dynamic load-relaxation data shown in Fig. 6 is plotted in Fig. 7. The scatter in the data is attributable to the previously mentioned noise. The same specimen was then remeasured in a static load-relaxation test at lower strain rates. A slight increase in the plastic strain resulted from loading in this static load-relaxation test. The appropriate equation from Hart's model [17] was used to fit the data. The expected $\dot{\epsilon}(\sigma)$ relationship for this material and temperature is given by

$$\dot{\epsilon} = \dot{a}^* \left(\frac{\sigma - \sigma^*}{G} \right)^M, \quad (4)$$

where \dot{a}^* is a rate parameter, G is the shear modulus, and M is a constant. Equation 4 was fitted to the low strain-rate data by adjusting σ^* , \dot{a}^* , and M . The resulting curve is shown in Fig. 7. It is clear that the medium strain-rate dynamic load-relaxation data is in reasonable agreement with the behaviour predicted by Hart's model when extrapolated from low strain rates.

Because the total imposed strains were small in the present investigation the effects of tempera-

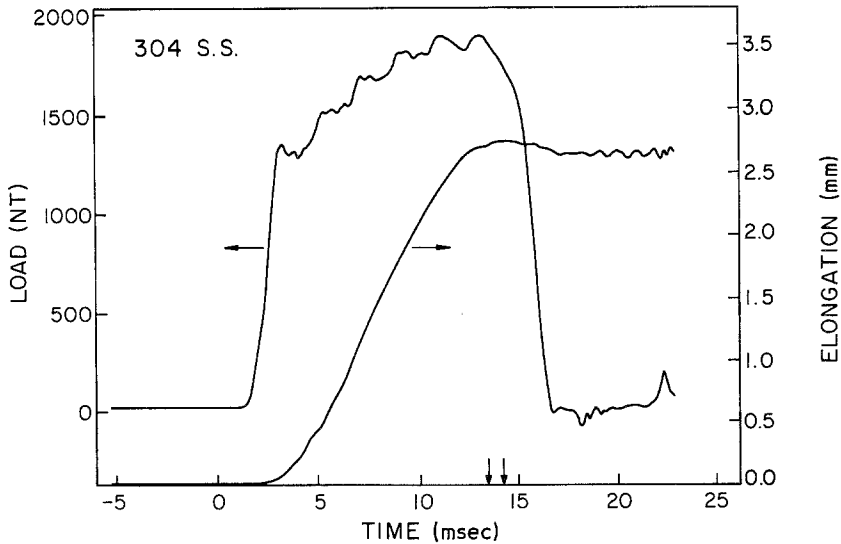


Figure 6 Curves of experimentally measured load plotted against time and specimen elongation plotted against time for type 304 stainless steel in a dynamic load-relaxation test.

ture changes were neglected in relating the low strain-rate and medium strain-rate relaxation data.

5. Conclusions

These preliminary experiments indicate that the dynamic load-relaxation test is feasible. The strain-rate range accessible for measurement is significantly higher than that for a static (conventional) load-relaxation testing procedure. The dynamic load-relaxation test is very rapid and thus the relaxation itself is essentially an adiabatic experiment. The amount of plastic deformation which

is imposed on the sample in order to measure a strain rate change of significant size is somewhat higher than that typically associated with a static load-relaxation test.

Hart's model was originally developed as a phenomenological description of plastic deformation of polycrystalline materials and was based on low strain-rate experiments. These preliminary dynamic load-relaxation experiments indicate that Hart's model may be valid over a much larger strain-rate range than has previously been experimentally shown.

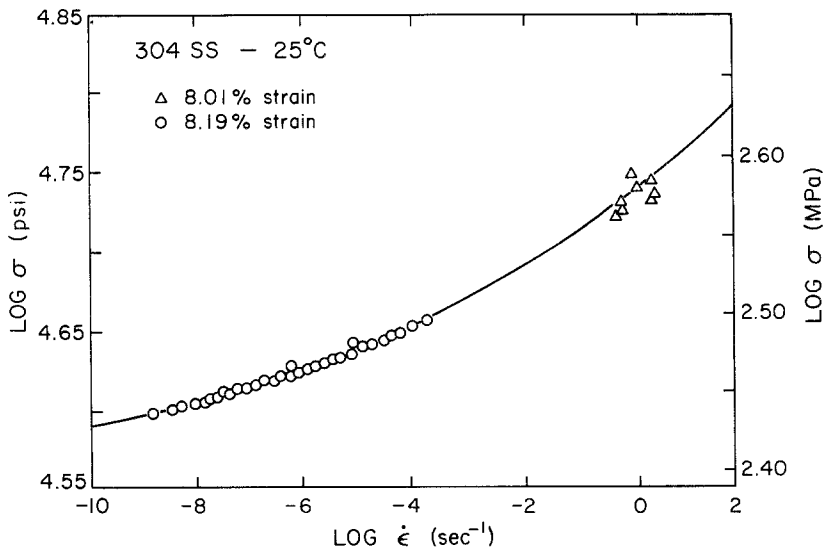


Figure 7 Curve of log stress against log strain rate for type 304 stainless steel. Data shown for a constant plastic state. Solid line shows best low strain-rate fit for Hart's model.

Acknowledgement

This work was supported by the Materials Science Division of the United States Department of Energy.

Appendix

Equation 1 is a quasistatic approximation and is valid when the time rate of change of the load, P , is sufficiently small that inertial effects can be neglected. The quasistatic approximation is valid if the two following criteria are met.

1. In order to achieve an elastic, quasistatic force distribution in the specimen, the load P must vary slowly compared to the transit time associated with the propagation of an elastic wave through the specimen. This criterion is required because both plastic and elastic waves propagate at the same velocity [12]. For a 2.54 cm (1 in.) long specimen and velocity of sound of $5 \times 10^3 \text{ m sec}^{-1}$, the transit time is approximately $5 \times 10^{-6} \text{ sec}$. These values are typical of most metals of technological interest.

2. In addition to the above elastic criteria, the load, P , varies over the length of the specimen if the moving member of the test machine is accelerated because the specimen itself is being accelerated.

Fig. 8 shows a tensile specimen of instantaneous length, L_T . One end of the specimen is fixed and the other end moves as a consequence of being attached to the moving member of the tensile machine. The difference in load applied

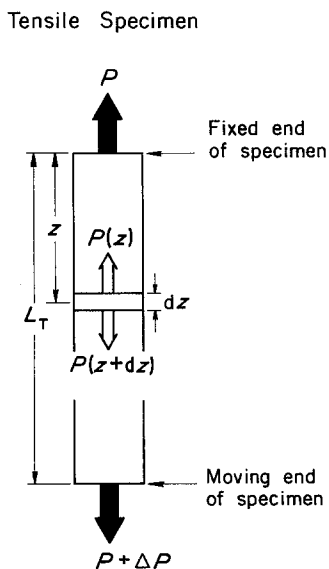


Figure 8 Schematic drawing of tensile specimen showing the variation of the load, P , with position, Z .

between the ends of the specimen, ΔP , occurs because of the acceleration of the specimen imposed during a tensile testing procedure. z defines the position of the volume element $A dz$, where A is the area of the specimen. The acceleration of this volume element requires that

$$dP = P(z) - P(z + dz) = a\rho A dz,$$

where dP is the net force experienced by the volume element, a is the acceleration of the volume element, and ρ is the mass density of the material comprising the specimen.

If criterion 1 is met and homogeneous deformation is assumed, then the acceleration of a volume element at point Z is given by

$$a = \frac{z}{L_T} \ddot{L}_T$$

where L_T is the total acceleration of the end of the specimen which is imposed by the testing machine. Thus, the difference in load, ΔP , between the ends of the test specimen is given by

$$\Delta P = \int_P^{P+\Delta P} dP = \int_0^{L_T} \frac{\rho A \ddot{L}_T}{L_T} z dz$$

$$\Delta P = \frac{\rho A L_T \ddot{L}_T}{2}.$$

ΔP must be small compared to the load, P , for the quasistatic approximation to hold. In the context of load-relaxation testing, ΔP must be small compared to the load changes required to produce significant changes in strain rate. If this is true, then the state of stress in the specimen can be assumed to be homogeneous.

References

1. E. OROWAN, British Iron Research Association Report No. MW/F/22/50 (1950).
2. J. F. ALDER and V. A. PHILLIPS, *J. Inst. Metals* 83 (1954-5) 80.
3. P. M. COOK, Proceedings, Conference on the Properties of Materials at High Strain Rates, (Institute of Mechanical Engineers, London, 1957).
4. J. E. HOCKETT, *Proc. ASTM* 59 (1959) 1309.
5. *Idem*, "Applied Polymer Symposia, High Speed Testing VI: The Rheology of Solids" (Interscience, New York) p. 205.
6. U. S. LINDHOLM and L. M. YEAKLEY, *Exp. Mech.* 7 (1967) 1.
7. *Idem*. AFML-TR-71-149 (1971) (Wright-Patterson Air Force Base, Ohio: Air Force Materials Laboratory).
8. B. LENGYEL and M. MOHITPOUR, *J. Inst. Metals* 100 (1972) 1.

9. R. L. WOODWARD and R. H. BROWN, *Proc. Inst. Mech. Eng.* **180** (1975) 107.
10. A. J. HOLZER, *Int. J. Mech. Sci.* **20** (1978) 553.
11. F. E. HAUSER, *Exp. Mech.* **6** (1966), 395.
12. J. D. CAMPBELL, *Mat. Sci. Eng.* **12** (1973) 3.
13. J. DUFFY, Proceedings of the Conference on Mechanical Properties of Materials at High Rates of Strain, Oxford, The Institute of Physics Conference Series No. 21 (1974) p. 72.
14. E. W. HART, *Acta Metall.* **15** (1967) 351.
15. D. LEE and E. W. HART, *Met. Trans.* **2** (1971) 1245.
16. P. ALEXOPOULOS, R. L. KEUSSEYAN, G. L. WIRE and C. Y. LI, ASTM Special Technical Publication 765.
17. E. W. HART, *Nuclear Eng. Design* **46** (1978) 179.

*Received 20 March
and accepted 31 May 1984*